

Opening Enediyne Scissors Wider: pH-Dependent DNA Photocleavage by *meta*-Diyne Lysine Conjugates[†]

Kemal Kaya, Madeleine Johnson and Igor V. Alabugin*

Department of Chemistry and Biochemistry, Florida State University, Tallahassee, FL

Received 15 October 2014, accepted 10 December 2014, DOI: 10.1111/php.12412

ABSTRACT

Photochemical activation of *meta*-dienes incapable of Bergman and C1–C5 cyclizations still leads to efficient double-strand DNA cleavage. Spatial proximity of the two arylethynyl groups is not required for efficient DNA photocleavage by the enediyne-lysine conjugates. Efficiency of the cleavage is a function of the external pH and DNA damage is strongly enhanced at pH < 7. The pH-dependence of the DNA photocleavage activity stems from the protonation states of lysine amino groups, the internal electron donors responsible for intramolecular PET quenching and deactivation of the photoreactive excited states. DNA-binding analysis suggests intercalative DNA binding for phenyl substituted conjugate and groove binding for TFP-substituted conjugate. Additional insights in the possible mechanism for DNA damage from the ROS (Reactive Oxygen Species) scavenger experiments found that generation of singlet oxygen is partially involved in the DNA damage.

INTRODUCTION

The ability of natural enediynes (1), hailed as the Nature's "most potent cancer agents" (2), to induce cleavage of both strands of a DNA duplex stems from the formation of a reactive *p*-benzyne diradicaloid via Bergman cyclization (3). Presence of two radical centers allows the initiation of hard-to-repair double-stranded DNA cleavage via two H abstractions from the DNA backbone. This chemistry inspired the development of new cancer therapies based on the controlled creation of either chemical (4) or photochemical DNA damage (5,6). Soon after the report of photo Bergman cyclization by Turro and Evenzahav (7), we found that increase in the acceptor power of terminal substituents enables C1–C5 cyclization of enediynes (8) initiated by the photoinduced electron transfer (PET) (Scheme 1).

Because the latter process leads to four formal H-transfers to the enediyne, it increases the DNA-damaging ability of this functional group even further (9). We had further amplified the potential of the photochemically activated enediynes by equipping them with pH-regulated amino acid functionality with variable protonation states (10). Although several amino acid/enediyne hybrids (11,12) have been reported in the literature (13,14) and the list is growing (15–17), we found the unique

advantage of lysine groups for the control of reactivity and biological utility of such hybrids. Not only do the positively charged amino acid residues allow to modulate binding with an anionic target such as DNA but they also allow to control photophysics of the enediyne chromophore via pH-gated intramolecular photoinduced electron transfer (PET). These conjugates are able to selectively cleave at G-sites flanking A-T tracks (18), convert nicked (ss) DNA into linear (ds) DNA (19) and induce intracellular DNA damage (20). Further modifications of the DNA binding and pH-regulating amino acid part of the hybrid molecules lead to highly efficient ds DNA photocleavage (21).

The above structural and functional features are especially interesting because the selectivity of natural enediynes toward cancer cells is low. Increasing the selectivity is the key requirement because damage to DNA of the healthy cells needs to be avoided. Furthermore, the parent enediyne system is relatively unreactive. Its activation via thermal Bergman cyclization requires a well-designed combination of strain and electronic effects (22). Computations have revealed that activation barrier of the Bergman cyclization could be decreased when appropriate cationic groups, i.e. protonated amines, are attached to enediynes (23). This finding introduces a possibility of selective targeting of cancer tissues via pH-regulated activation of a prodrug.

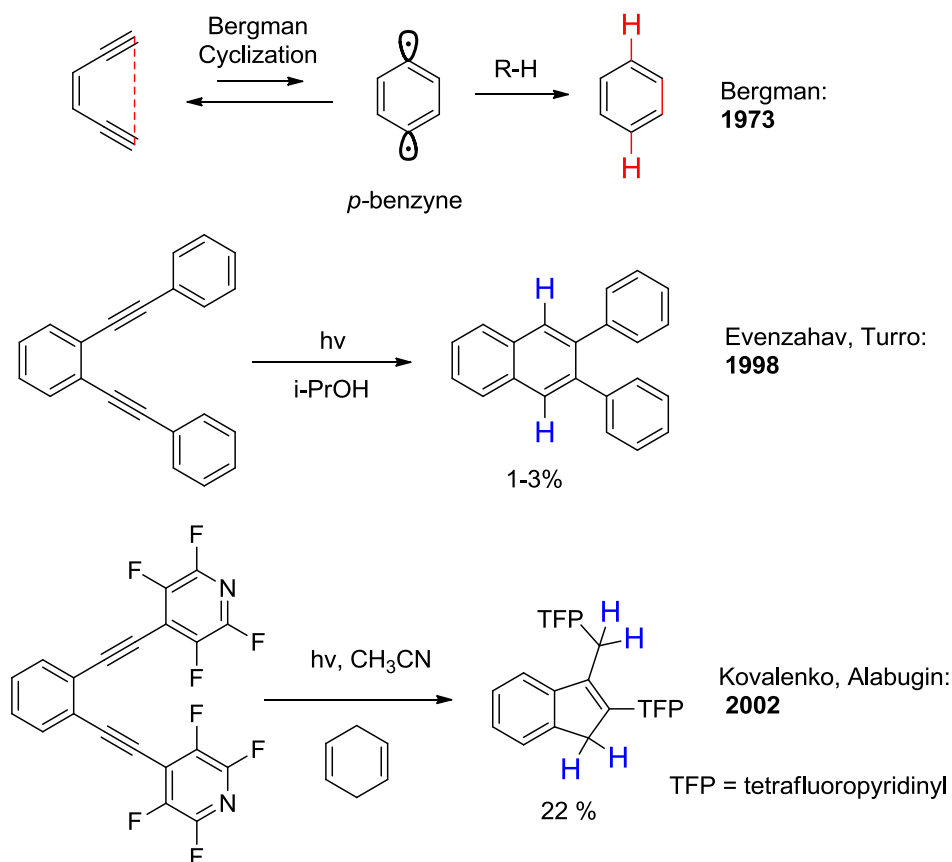
More than 80 years ago, Warburg showed that tumor cells actively convert glucose and other substrates to lactic acid with the concomitant decrease in the pH (24). Most of the additional H⁺ ions are transported outside of the cell, so it is the extracellular environment that acidified the most. However, it is possible to equilibrate the extracellular H⁺ ions with the cell contents (25,26), thus lowering intracellular pH of cancer cells, using certain drugs such as amiloride (27,28), nigericin (29) and hydralazine. Under such conditions, one can take advantage of the acidic environment of cancer cells for the design of chemical agents that increase reactivity and selectivity at the lower pH (30).

In the efforts to better understand the photochemistry and photophysics responsible for the highly efficient DNA cleavage, Yang *et al.* (10) discover surprising DNA photocleavage activity of the mono acetylene-lysine conjugates (Fig. 1). Because monoalkynes can undergo neither Bergman nor C1–C5 cyclization, DNA cleavage by these molecules is likely to originate from a combination of photoinduced electron transfer (PET) and base alkylation. To gain better understanding of structural effects in the observed photochemistry, we tested the relative reactivity of the excited *o*-, *m*- and *p*- acetamidyls towards 1,4-cyclohexadiene (1,4-CHD) as a reactive π -system that mimics DNA bases as

*Corresponding author email: alabugin@chem.fsu.edu (Igor V. Alabugin)

[†]This manuscript is part of the Special Issue dedicated to the memory of Michael Kasha.

© 2014 The American Society of Photobiology



Scheme 1. Thermal Bergman cyclization, photochemical Bergman cyclization and C1-C5 cyclization.

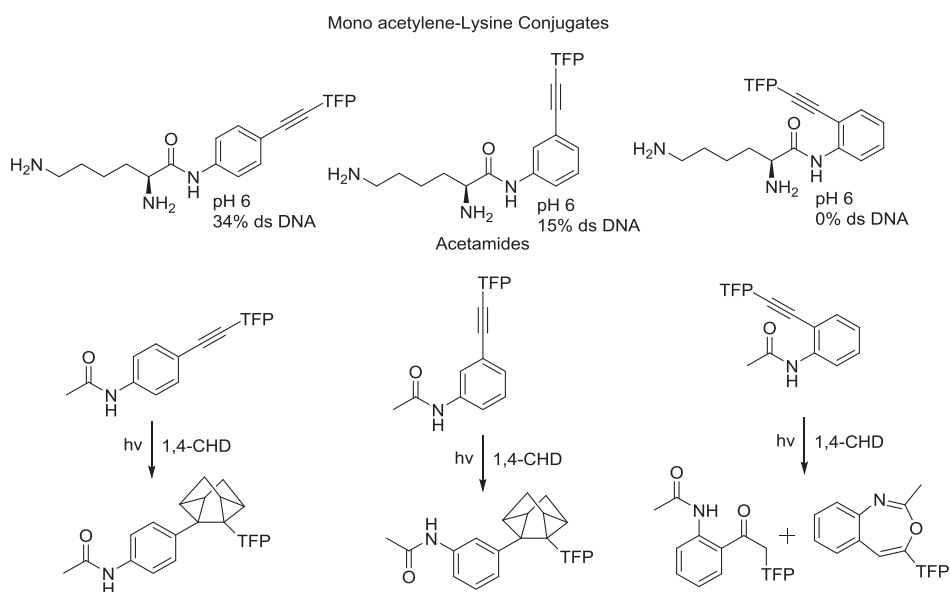


Figure 1. Isomeric acetylene-lysine conjugates and respective acetanilides.

well as serve as both the electron and H-atom donor toward the excited alkynes (31). This study found that both *p*- and *m*-acetamidyls alkylate 1,4-CHD to form the formal photocycloaddition product whereas *o*-isomer gave the products of intramolecular cyclization. In parallel, we found that only the *p*- and *m*-alkyne

isomers were capable of causing the ds DNA cleavage. Encouraged by the correlation between DNA-cleaving ability of mono-alkynes and their alkylating properties and by observation of DNA photocleavage activity of the *m*-acetylene-lysine conjugate, we decided to look deeper at the use of metasubstituted alkynes

in the design of light-activated reagents for the ds DNA cleavage.

Considering that the ortho alkynes are unreactive, there are the two possible ways to place two alkyne groups at a benzene core position which does not interfere with DNA photocleavage. Whereas the *m,p*-isomer corresponds to the well-explored enediyne that can react via Bergman and C1–C5 cyclization, the second (*m,m*) isomer has not been tested in photoreaction with DNA before. Taking into account the substantial effects of *m*-substitution on photochemical processes (32,33), the *m,m*-isomer is an interesting choice in the design of DNA photocleavers. This structural modification keeps the total number of alkynes the same as in the commonly studied enediyne but, at the same time, it changes molecular shape, moves both alkynes closer to the DNA-binding group, and spatially separates the alkynes, eliminating the possibility of both the Bergman and C1–C5 cyclizations.

Considering these factors and sensitivity of DNA binding to the shape of the DNA cleaver, we decided to investigate the pH-dependent binding and photoreactivity of the *m,m*-isomer. We can further vary the electron acceptor ability and the electrophilicity of the DNA-damaging warheads by changing substitution at the terminal position of alkynes. In this work, we included bis-alkynes with either phenyl (Ph) or a strong electron acceptor group tetrafluoropyridyl (TFP) at the remote alkyne termini (Fig. 2).

MATERIALS AND METHODS

General information. All chemicals were purchased the highest purity available and the reactions were performed under dry N₂. Purification of the products and synthesized intermediates was performed using silica (60 Å, 230–400 mesh). ¹H and ¹³C NMR spectra were collected on a Bruker 400 MHz and 600 MHz NMR spectrometer. Individual solvent signals were assigned as reference chemical shift. Mass spectrometry data were collected on a Jeol JMS-600H. UV spectra were recorded on Agilent Cary 60 UV-Vis Spectrophotometer. The fluorescence spectra were collected on a Fluorolog-3 spectrometer (Jobin Yvon Inc., Edison, NJ) equipped with TBX PMT detector and an air cooled CCD camera. pH was adjusted with AB 15 plus pH meter (Accument) after standardization at 25°C. All buffers were prepared and pH-adjusted at room temperature (25°C).

Plasmid DNA photocleavage. pBR322 plasmid DNA (4361 b/p; from BioLabs Inc., 1 μg μL⁻¹ solution in 10 mM Tris-HCl (pH 8.0), and 1 mM EDTA buffer) was diluted to a concentration of 0.01 μg μL⁻¹. The solution containing cleavage agent, DNA (30 μM bp⁻¹) in 20 mM sodium phosphate buffer was incubated for 1 h at 30°C. Samples were placed on ice at a distance of 20 cm from 200 W Hg-Xe lamp (Spectra-

Physics, Laser & Photonics Oriel Instruments with long pass filter with 324 nm cut-on wavelength).

Electrophoretic analysis. The gel electrophoresis was carried out in 1× TBE buffer at 80 V using Miligel FisherBiotech Horizontal Electrophoresis System. All gels were run on 1% agarose slab gels. Before loading, the DNA samples were mixed with 0.33 volume of tracking dye containing bromophenol blue (0.25%) and glycerol (30%) in water. After staining in ethidium bromide solution (2 μg mL⁻¹) for 3 h, the gel was washed with water and pictures were taken. The relative quantities of the supercoiled, nicked and linear DNA were calculated by integrating the “area” of each spot by the image analyzer software Total/Lab (Nonlinear Dynamics Ltd., UK). The amount of supercoiled DNA was multiplied by factor of 1.4 to account for reduced ethidium bromide intercalation into supercoiled DNA.

Spectrometric determinations of p*K_a*. pH of 15 μM of compound solution in H₂O was adjusted with 0.1, 0.2, 1.0 M HCl (aq) and NaOH (aq) solution. UV spectra were recorded for each titration point. Quartz cuvettes were used.

Absorbance titration with DNA. Two milligram of calf thymus DNA was dissolved in 1.5 mL of double distilled water and the concentrations of calf thymus DNA stock solution was determined spectrophotometrically using the following molar absorptivity value: 13 200 M⁻¹ cm⁻¹ (per base pair) at 260 nm. All experiments were carried out in 20 mM sodium phosphate buffers at 25°C and quartz cuvettes were used. The same amount of DNA was added to both sample and reference cuvettes during UV/Vis titration.

Fluorescence titration with DNA. The solution of 15 μM compound in 20 mM sodium phosphate buffers were titrated by adding (0–10.8 μM [base pair]) ct DNA. Fluorescence spectra were recorded for each measurement. Quartz cuvettes were used.

Ethidium bromide displacement. The concentration of ethidium bromide was determined spectrophotometrically using the molar absorptivity value: 5.60 × 10³ M⁻¹ cm⁻¹ at 480 nm. The solutions of 10 μM ethidium bromide and 10 μM ct DNA in 20 mM sodium phosphate buffer are tested by adding 1.5 μL of compounds solution (1 mM) each time. The experiments were carried out at 25°C and PMMA cuvettes were used. Emission was measured 10 min. after addition of compound to get the equilibrium.

RESULTS AND DISCUSSION

Synthesis

Sonogashira cross coupling of 3,5-dibromonitrobenzene with trimethylsilyl (TMS) acetylene and phenyl acetylene produced compounds **4** and **5**. The substitution of **5** with tetrafluoropyridyl (TFP) group was achieved using CsF promoted reaction with pentafluoropyridine (PFP). Reduction in nitro groups of **4** and **6** with SnCl₂ yielded anilines **7** and **8**. Compound **7** can be coupled with Boc-protected lysine in POCl₃ to produce the conjugate **10**. The more reactive aniline **7** undergoes reaction with Boc-protected lysine in the presence of 1-ethyl-3-(3-dimethylaminopropyl)

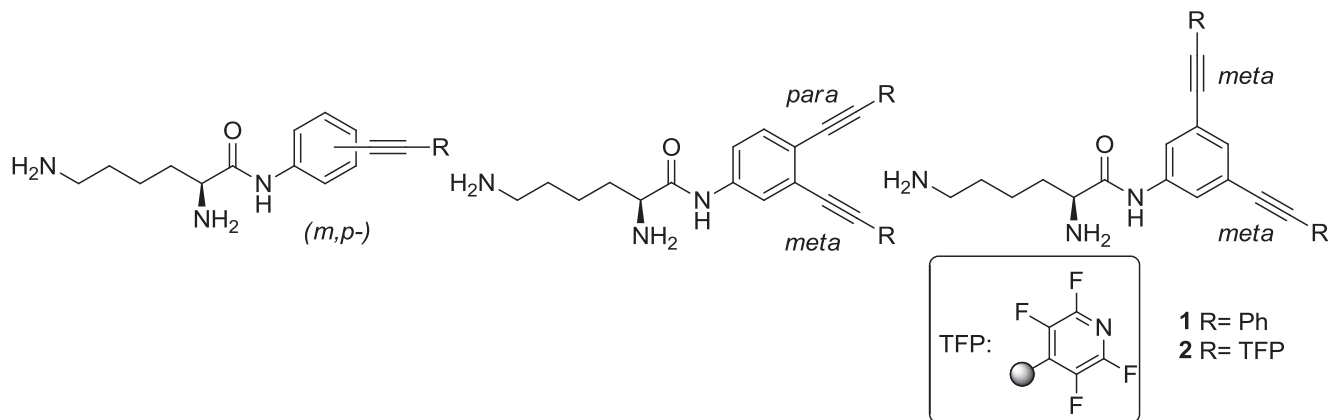


Figure 2. Evolution of molecular design of lysine-alkyne conjugates.

carbodiimide (*EDCI*) and 1-hydroxybenzotriazole (*HOBt*) as coupling reagents to yield **9**. The removal of Boc groups with trifluoroacetic acid in dichloromethane produced the target conjugates **1** and **2** as water-soluble TFA salts (Scheme 2).

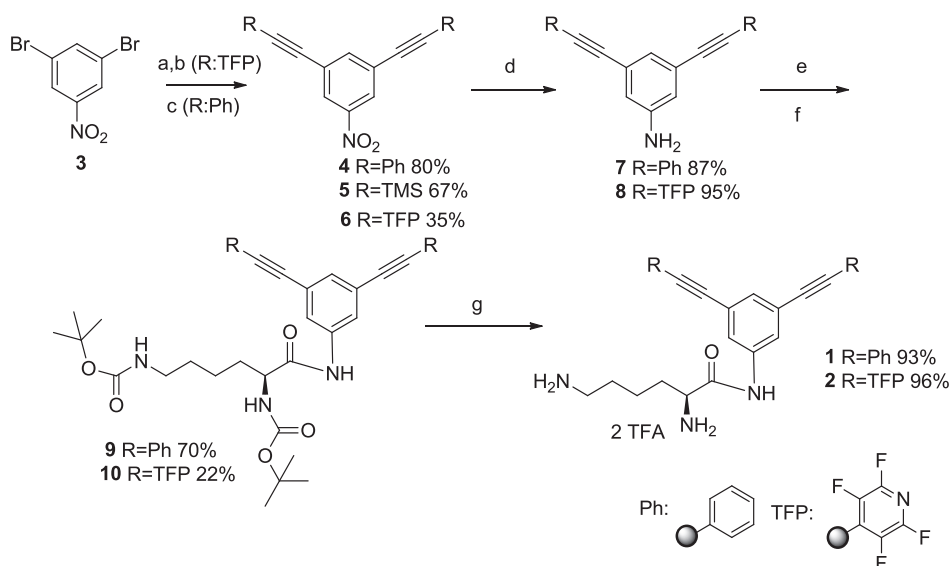
Photophysical properties

Determination of pK_a . To test whether the new conjugates are suitable for the pH-regulated DNA cleavage, the pK_a values of the conjugates were studied by UV spectroscopy. UV spectroscopy is a useful method for determination of acid dissociation constant (pK_a) of the compounds (34). If the chromophore is sufficiently close to the ionization center, the protonated and deprotonated forms of the compounds will have adequate spectral differences (35,36). 15 μM aqueous solutions of each compound were titrated with 0.1, 0.2 and 1.0 M HCl and NaOH with the intermediate pH values measured by AB15+ pH Meter. The UV spectrum of the compounds was taken for each point of titration (Fig. 3). The change in absorbance is plotted against pH and data are fitted to Henderson–Hasselbalch equation.

The obtained pK_a values for each compound are shown in Fig. 4. pK_a of conjugate **1** is 7.5 and pK_a of conjugate **2** is 7.3.

The absorbance of the bis-Ph diyne **1** changed in a systematic way with a clearly defined isosbestic point. On the other hand, the spectra of the bis-TFP analog **2** changed in a more complex way where the initial spectral evolution that was similar to that for compound **1** changed at $\sim\text{pH}$ 9.0 to give rise to the formation of a broader redshifted absorbance. Such changes may indicate the beginning of aggregation at the higher pH where transformation of cations into neutral species starts to become sufficiently important. Despite the differences in the spectral behavior, the pK_a values for the two compounds are similar. This similarity is expected because of **1** and **2** differ only at substitution of the remote terminal position of the alkyne moiety. Translocation of *p*-alkyne in *m,p*-enediynes hybrids to the meta position, significantly alleviates the acidifying effect of the acceptor TFP group at the α -amino group of lysine.

Because the ϵ -amino group of lysine is far away from the chromophore, we assume that the measured pK_a value corresponds to α -amino group of each lysine conjugates. Indeed, very small spectral changes are observed at the higher pH where deprotonation of the ϵ -ammonium is expected. The pK_a values suggest that the amino groups of compounds will be >50% protonated below pH 7.4 (37). Below pH 6.4, >90% of the



Scheme 2. Synthesis of lysine-bisacetylene conjugates.

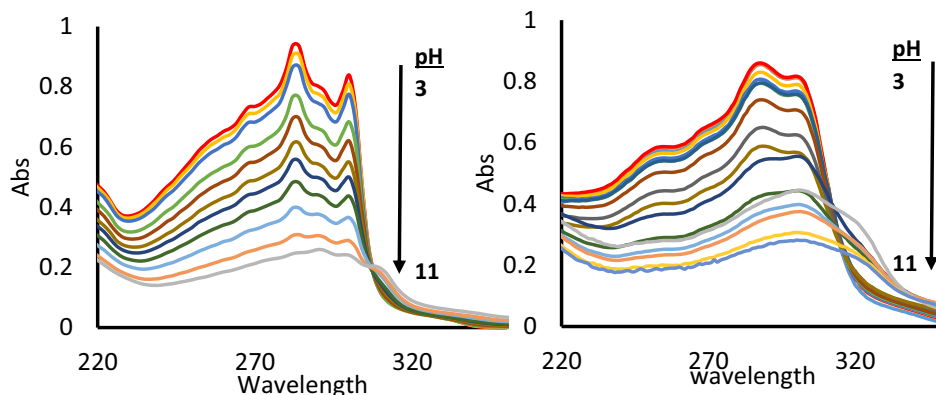


Figure 3. Changes in UV spectra during pH titration of the conjugates **1** (left) and **2** (right).

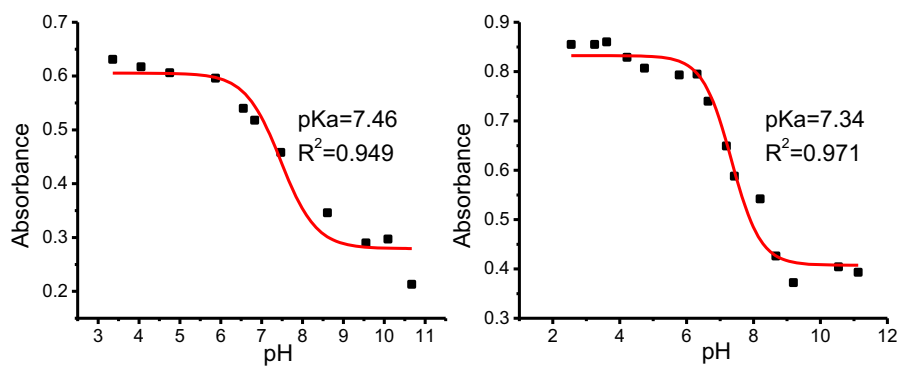


Figure 4. pKa values of compound **1** (left) and **2** (right) obtained from UV absorbance.

self-quenching PET from the lone pair of α -amino group to the excited chromophore will be blocked.

DNA binding

Small molecules can interact with DNA via several modes such as electrostatic interactions, groove binding and intercalation (38). To study interaction of our compounds with DNA, we titrated the conjugates with Calf Thymus DNA (ct DNA) at different pH conditions and the binding constants of the conjugates

with DNA were determined from UV spectra using the Eq. 1 (39).

$$[\text{DNA}]/(\epsilon_a - \epsilon_f) = [\text{DNA}]/(\epsilon_b - \epsilon_f) + 1/K_b(\epsilon_b - \epsilon_f) \quad (1)$$

where ϵ_a is apparent extinction coefficient of complex with DNA, ϵ_b is extinction coefficient of fully bound complex, ϵ_f is extinction coefficient of unbound compound and K_b is the DNA-binding constant of the compound. $[\text{DNA}]/(\epsilon_a - \epsilon_f)$ is plotted vs

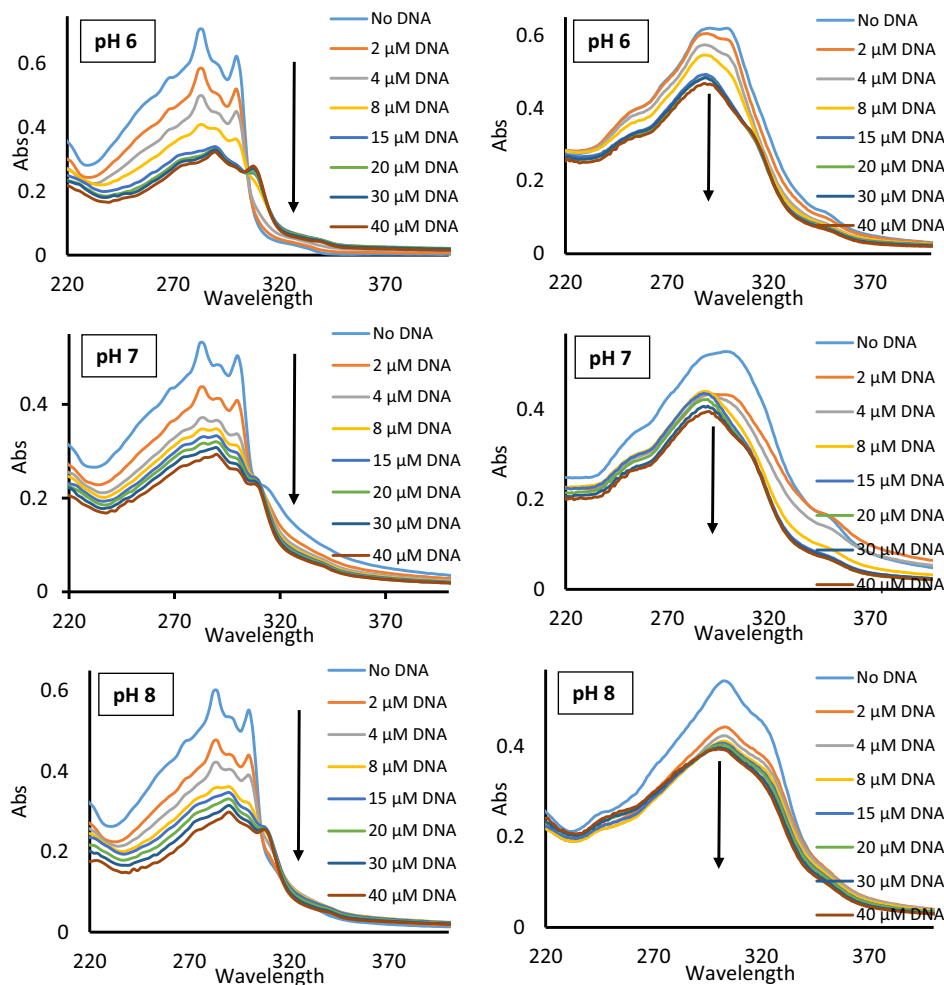


Figure 5. Changes in UV spectra of the compounds **1** (left) and **2** (right) with addition of ct DNA (0, 2, 4, 8, 15, 20, 30 and 40 μM , respectively, arrows show the increasing amount of ct DNA) (20 mM) at different pH.

[DNA] and slope is divided by y -intercept gave the (K_b) binding constant.

Both compounds show significant UV absorption at ~ 300 nm in the absence of DNA (Fig. 5). With addition of 0–40 μM ct DNA, the absorbance intensity steadily decreases. Such hypochromic behavior with the concomitant bathochromic shift is often taken as a strong evidence for intercalation with DNA (40). It is generally attributed to the decrease in the HOMO-LUMO gap of π - π^* excitation state as the molecules intercalate between the DNA base pairs (38,41). In the case of conjugate **1**, the large hypochromicity (54% at pH 6, 50% at pH 7 and 45% at pH 8), bathochromic shift (8 nm) supports intercalation with DNA. Furthermore, the binding constants of the compound **1** are closer to each other for all pH conditions (Table 1), indicating that the binding mode of the compound **1** is insensitive to acidity of solution and protonation states of the lysine chain. On the other hand, conjugate **2** is much more sensitive to the different pH conditions and displays stronger binding constants at the higher pH values. The absence of an isosbestic point shows that binding mode of the conjugate **2** to DNA is not a simple process but rather involves an evolving assemble of species of different nature. The small hypochromicity (30% at pH 6, 24% at pH 7 and 28% at pH 8) and absence of the redshift argue against intercalation of compound **2**. Remaining possibilities include electro-

static interaction with the phosphate backbone or binding at the DNA grooves. At lower pH, electrostatic interaction between phosphate backbone of the DNA and the ammonium groups of the lysine should be favorable. However, conjugate **2** displayed stronger binding constants at the higher pH, when the α -ammonium group should lose its charge and the electrostatic interaction with phosphate backbones of DNA should weaken. This finding suggests that the likely binding mode for conjugate **2** involves groove binding. The latter can be more favorable when α -ammonium loses its charge at the higher pH values since conjugate **2** becomes more hydrophobic. In an aqueous solution, the hydrophobic moiety (chromophore) of the molecule will have stronger affinity toward the DNA grooves.

Competitive DNA binding with ethidium bromide

To gain further insight in the mode of DNA binding for the two conjugates, we investigated competitive DNA-binding study with ethidium bromide (EB), a well-studied DNA intercalator. The DNA-binding constants obtained from the UV absorption spectra (previous section) are comparable with those for the number of DNA intercalators reported in the literature (10^5 – 10^{11} M^{-1}) (42). The EB displacement assay is commonly used as an indicator for intercalation due to the large decrease in EB fluorescence

Table 1. Summary of DNA-binding constants. The values in parenthesis show the standard deviation of three individual experiments.

Compound	pH 6	pH 7	pH 8	Compound	pH 6	pH 7	pH 8
	$K_b, 10^5 \text{ M}^{-1}$	$K_b, 10^5 \text{ M}^{-1}$	$K_b, 10^5 \text{ M}^{-1}$		$K_b, 10^5 \text{ M}^{-1}$	$K_b, 10^5 \text{ M}^{-1}$	$K_b, 10^5 \text{ M}^{-1}$
1 (284 nm)	2.5 (± 0.5)	2.2 (± 0.3)	2.8 (± 0.2)	2 (299 nm)	1.1 (± 0.1)	4.3 (± 0.8)	9.0 (± 1.4)
1 (300 nm)	2.0 (± 0.0)	2.5 (± 0.0)	2.7 (± 0.3)				

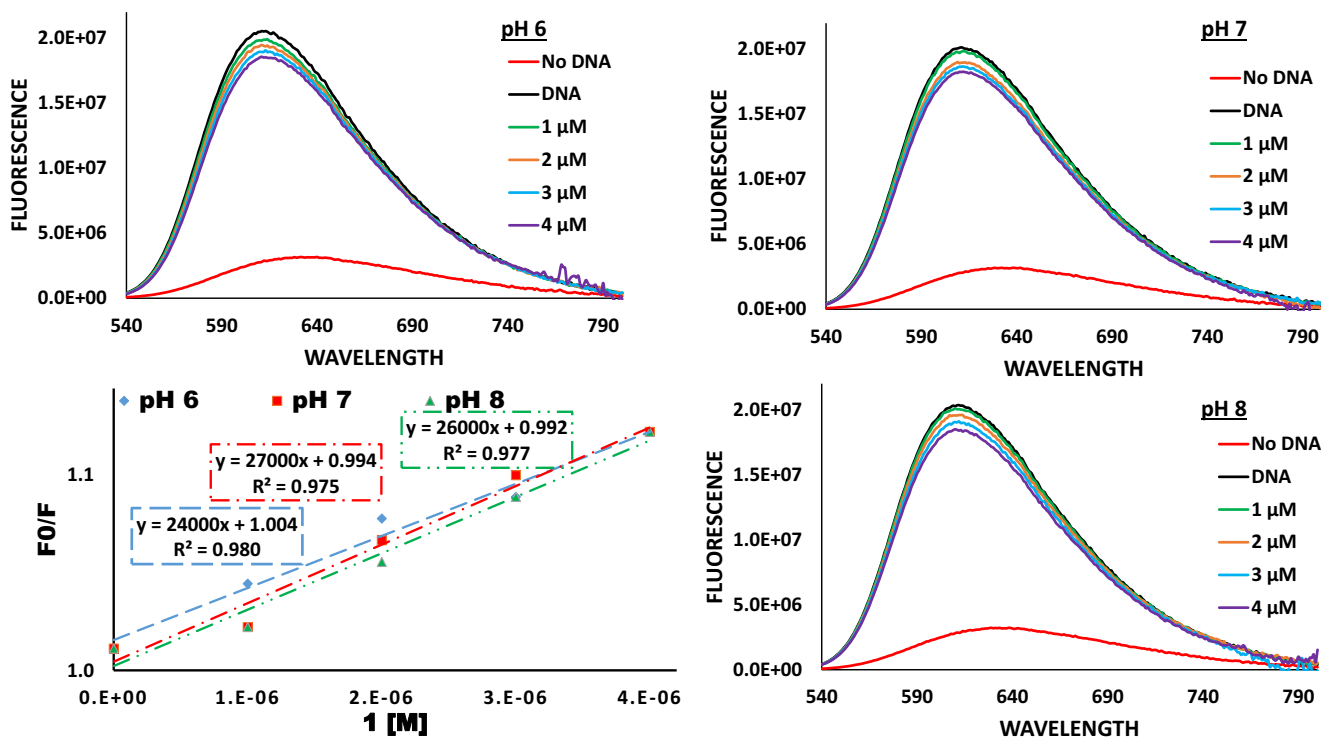


Figure 6. Changes in fluorescence of ethidium bromide upon its displacement from ct DNA by compound **1** (excitation wavelength is 525 nm).

intensity as it is displaced from DNA into aqueous environment (43).

To study competitive binding ability of the compound with EB, we titrated DNA-ethidium bromide (DNA-EB) complex with compounds **1** and **2** for different pHs. For all the pH conditions, the compounds displace EB, leading to decrease in fluorescence intensity from the (EB-DNA) complex. As expected from the UV titrations, compound **1** has shown similar binding for all pH conditions as well as showing that DNA-binding mode of the compound **1** is a single-mode process (Fig. 6). Compound **2** displaced EB most efficiently at the lower pH whereas similar, less efficient, displacement was observed for pH 7 and pH 8 conditions (Fig. 7). This finding suggests that binding mode at low pH conditions is different than the higher pH conditions. UV titrations of the compound **2** and EB displacement experiment suggest that groove binding is the major interaction at higher pHs whereas intercalation becomes important at low pH.

Fluorescence

We investigated direct quenching of fluorescence of compound **1** with ct DNA as well. With addition of DNA, fluorescence intensity of the compound **1** decreases. Figure 8 shows the changes on the fluorescence and the respective Stern–Volmer plots for quenching of compound **1** with addition of DNA at pH 6 (see Supplementary Materials for pH 7 and pH 8). The quenching constants were calculated from the Stern–Volmer equation. F_0 and F are the fluorescence intensities of the compounds in absence and presence of different concentrations of ct DNA.

From the fluorescence data, the binding constants and binding stoichiometry for conjugates at different pH conditions can be

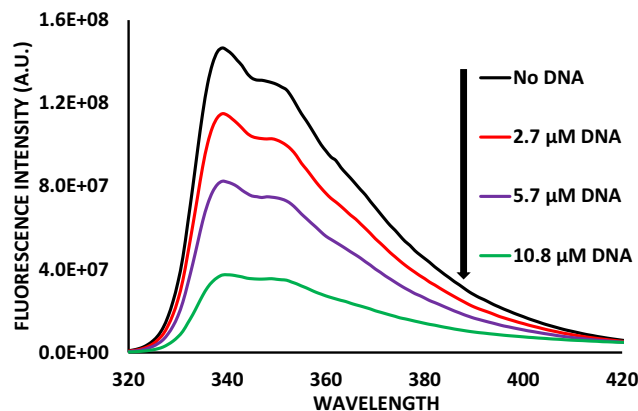


Figure 8. Fluorescence titration spectra of the compound **1** ($15 \mu\text{M}$) with ct DNA ($0\text{--}10.8 \mu\text{M bp}^{-1}$) at pH 6 (excitation at 307 nm).

calculated from Eq. 2 (44). K and n are the binding constant and number of binding sites, respectively.

$$\log[(F_0 - F)/F] = \log K + n \log[\text{DNA}] \quad (2)$$

Calculated binding constants are values close to each other for compound **1** at pH 6 and pH 7 conditions which is below the pK_a value (7.46) whereas it resulted in 10-fold less for pH 8 conditions which is higher than pK_a value of the compound **1** while quenching constants are similar for all pH conditions (Table 2).

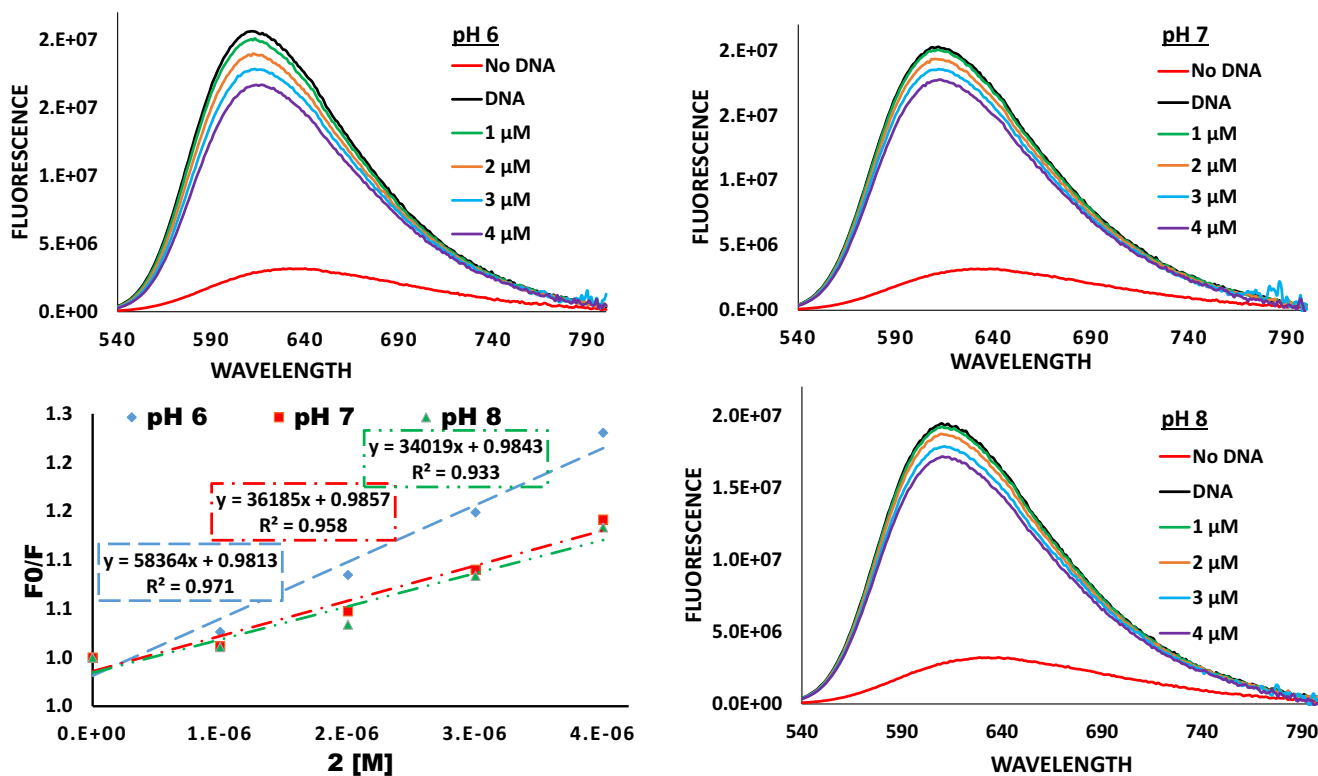


Figure 7. Changes in fluorescence of ethidium bromide upon its displacement from ct DNA by compound compound **2** (excitation wavelength is 525 nm).

Table 2. Binding and quenching constants of compounds.

Compound	$K_{sv} \times 10^5 \text{ M}^{-1}$	$K_b \cdot 10^7 \text{ M}^{-1}$	n
1 (pH 6)	3.34	3.09	1.42
1 (pH 7)	3.81	2.79	1.28
1 (pH 8)	3.38	0.41	1.21

Due to the absence of the isosbestic point during the titration of compound **2** with ct DNA, we have not performed the fluorescence titration for this compound with DNA.

DNA photocleavage

Encouraged by promising pKa values of the new conjugates for pH regulation, we evaluated DNA cleavage activity of

compounds using 15 μM of each compound and 30 μM (per base pair) of DNA for the biologically relevant pH conditions. The efficiencies of DNA photocleavage were monitored using the plasmid relaxation assays. Conversion of supercoiled plasmid DNA (Form I) into the respective relaxed circular and linear forms (Forms II and III) was determined by densitometric analysis of the gel electrophoresis bands.

In all pH conditions, Ph and TFP alkynes are able to generate ds DNA cleavage (Form III). Furthermore, both compounds are remarkably more active at lower pH (pH 6, conjugate **2** ss:ds 1.0:1.2). This behavior is associated with the basic properties of the α -amino group of the lysine moiety in the conjugates. Protonation of amino groups increases efficiency of DNA photocleavage (Fig. 9).

At lower pH, both amino groups will be protonated, thus, excited state reactivity is not quenched via intramolecular and intermolecular PET from the lone pair of α -nitrogen (Fig. 10).

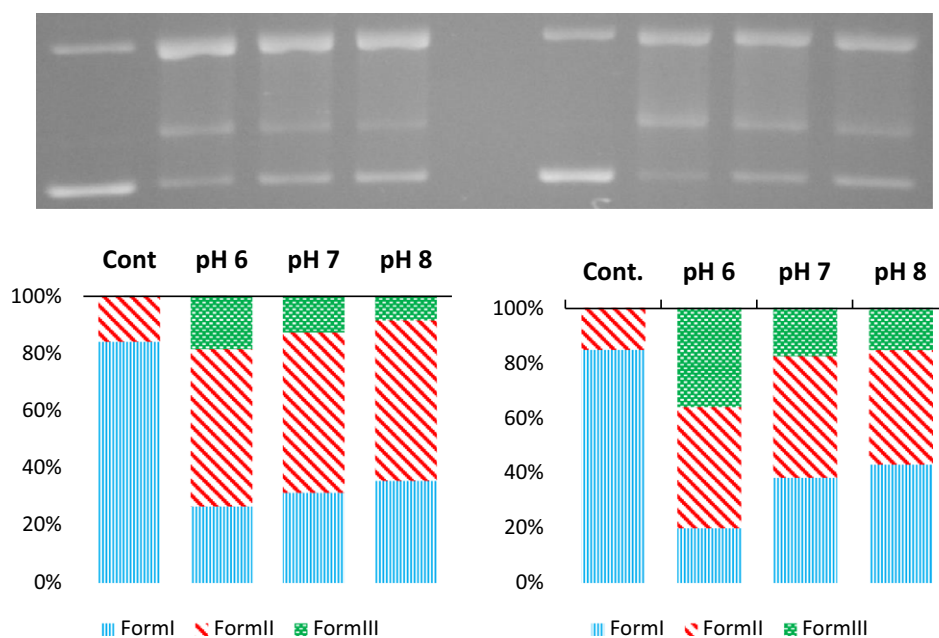


Figure 9. Ethidium bromide stained agarose gel image and quantified cleavage data for plasmid relaxation assay for DNA photocleavage with 15 μM of bis-acetylenic conjugates **1** (left) and **2** (right) and 30 μM (bp) of pBR322 plasmid DNA at pH range 6–8 after 10 min. of UV (>300 nm) irradiation. Reported values represent the average of three experiments.

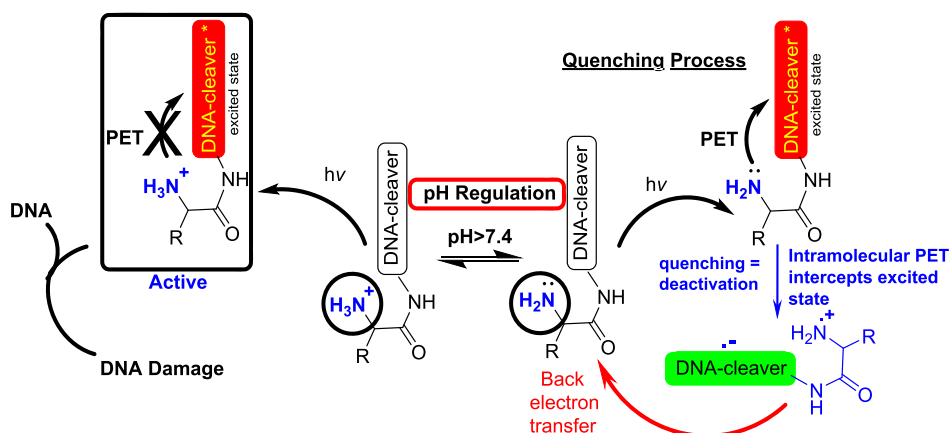


Figure 10. Activation and deactivation of pH-gated DNA photocleavage.

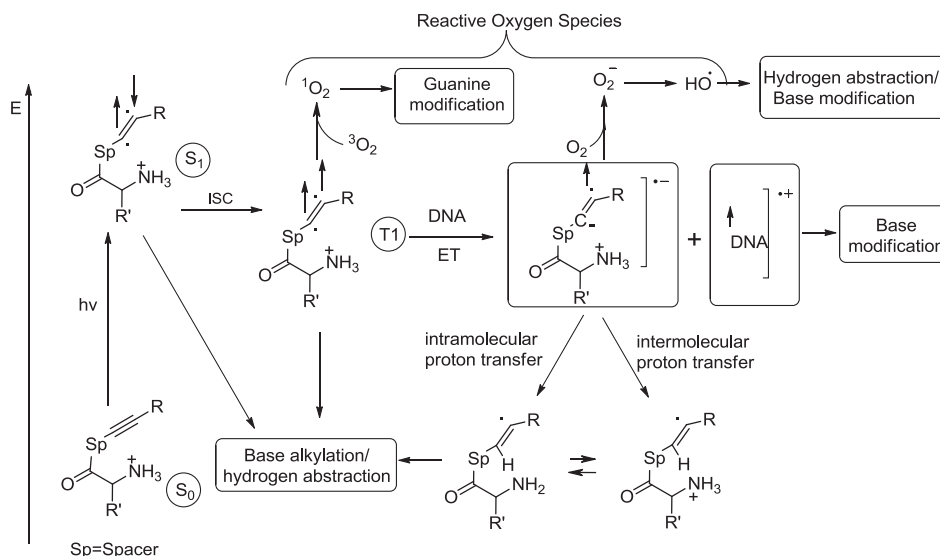


Figure 11. Possible mechanistic pathways for DNA photocleavage.

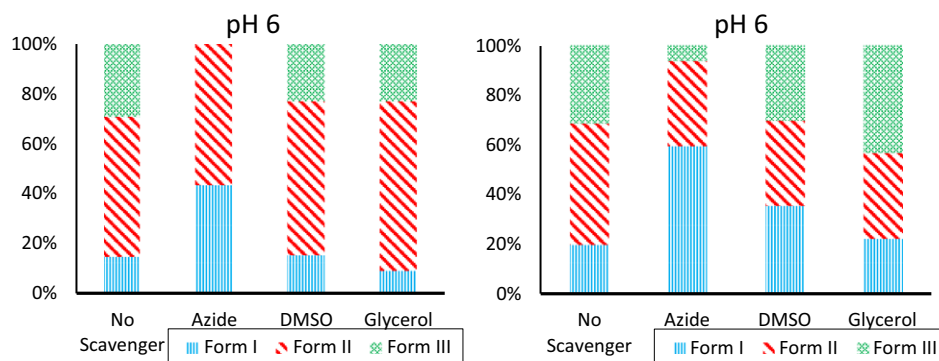


Figure 12. Effect of hydroxyl radical/singlet oxygen scavengers (20 mM) upon the efficiency of DNA cleavage at pH 6 by conjugates **1** and **2**.

When pH increases, the amount of unprotonated α -amino group of lysine grows, rendering PET from lone pair electrons of nitrogen possible. The charge-separated state can go back to the ground state after back electron transfer. The overall process is unproductive from the photochemical perspective and lead to the decreased reactivity of lysine conjugates toward DNA at the higher pH.

Scavenger experiments

In the absence of light, both conjugates do not induce DNA cleavage. Possible mechanistic scenarios for DNA damage by the conjugates can be summarized in Fig. 11 (45). Having acetylenes in the meta arrangement eliminates both the Bergman and C1–C5 cyclization but the number of other possibilities remain, such as cross-link formation between dipeptides and DNA, alkylation of DNA nucleobases (46,47) and their oxidative damage initiated by electron transfer (48–50), hydrogen abstraction from the sugar moieties (51,52) and other reactions with reactive oxygen species (ROS) (53–55).

Irradiation with UV light transforms the conjugates into the excited singlet states. The excited molecule can undergo intersys-

tem crossing (ISC) to generate triplet excited state. Both singlet and triplet states of alkynes possess sufficient electrophilicity for alkylating reactive π -systems and damaging DNA via base alkylation (56,57). In addition, the triplet state can sensitize the transformation of molecular oxygen into singlet oxygen (1O_2). The latter highly reactive form of oxygen can oxidize DNA bases, especially guanine. Another path to cleave DNA is via electron transfer (ET) from DNA generating alkyne radical anion, capable of transferring an electron to molecular oxygen with the formation of superoxide. The latter species can undergo further reactions to generate hydroxyl radical.

To investigate the possible involvement of reactive oxygen species (ROS), we used the selection of traps for different ROS, i.e. glycerol and DMSO (53,54) as hydroxyl radical scavengers and NaN₃ (55) as a singlet oxygen scavenger. The results of these scavenging experiments are summarized in Fig. 12.

Albeit there is no significant effect by hydroxyl radical scavengers (DMSO and glycerol) for both compounds, ds DNA photocleavage activity of the conjugate **2** is inhibited (70%) by singlet oxygen scavenger (NaN₃). This inhibition is even more pronounced for conjugate **1**, where singlet oxygen is responsible for significant part of DNA photocleavage.

CONCLUSIONS

Spatial proximity of two arylethynyl groups is not required for efficient DNA photocleavage by enediyne-lysine conjugates. Newly prepared meta-bis-alkyne chromophores are able to induce DNA ds-photocleavage upon UV irradiation at different pH conditions. Translocation of *p*-alkyne in *m,p*-enediyne hybrids to the meta position, alleviates the acidifying effect of the acceptor TFP group, rendering the α -amino group of lysine residues to have similar basicity in the two conjugates. The intrinsic DNA-binding constants of the conjugates from UV titrations suggest intercalative DNA binding for phenyl substituted conjugate (1) and groove binding for TFP substituted conjugate (2). The difference of the DNA photocleavage activity of the conjugates stems from protonation states of lysine amino groups, responsible for intramolecular PET quenching of excited state of molecules. Scavenger experiments for ROS has shown that generation of singlet oxygen is an important contributor to the observed DNA ds-damage.

Acknowledgements—This work was supported by the Natural Science Foundation (Grant CHE-1152491). The paper is dedicated to the memory of Professor Michael Kasha, an esteemed colleague whose intellectual generosity and quick wit illuminated so many discussions at the faculty coffee table in the Dittmer Chemistry Building at the Florida State University.

SUPPORTING INFORMATION

Additional Supporting Information may be found in the online version of this article:

Figure S1. Fluorescence titration spectra of the compound 1 (15 μM) with ct DNA (0–10.8 $\mu\text{M bp}^{-1}$) at pH 7 (excitation at 307 nm).

Figure S2. Fluorescence titration spectra of the compound 1 (15 μM) with ct DNA (0–10.8 $\mu\text{M bp}^{-1}$) at pH 8 (excitation at 307 nm).

Data S1. Synthesis of compounds.

REFERENCES

- Nicolaou, K. C., A. L. Smith and E. W. Yue (1993) Chemistry and biology of natural and designed enediynes. *Proc. Natl Acad. Sci. USA* **90**, 5881–5888.
- Galm, U., M. H. Hager, S. G. van Lanen, J. Ju, J. S. Thorson and B. Shen (2005) Antitumor antibiotics: Bleomycin, enediynes. *Mitomycin. Chem. Rev.* **105**, 739–758.
- Bergman, R. G. (1973) Reactive 1,4-dehydroaromatics. *Acc. Chem. Res.* **6**, 25–31.
- Stanulla, M., J. Wang, D. S. Chervinsky, S. Thandla and P. D. Aplan (1997) DNA cleavage within the MLL breakpoint cluster region is a specific event which occurs as part of higher-order chromatin fragmentation during the initial stages of apoptosis. *Mol. Cell. Biol.* **17**, 4070–4079.
- Armitage, B. (1998) Photocleav. Nucl. Acids. *Chem. Rev.* **98**, 1171–1200.
- Breiner, B., K. Kaya, S. Roy, W.-Y. Yang and I. V. Alabugin (2012) Hybrids of amino acids and acetylenic DNA-photocleavers: optimising efficiency and selectivity for cancer phototherapy. *Org. Biomol. Chem.* **10**, 3974–3987.
- Evenzahav, A. and N. J. Turro (1998) Photochemical rearrangement of enediynes: is a “Photo-Bergman” cyclization a possibility? *J. Am. Chem. Soc.* **120**, 1835–1841.
- Alabugin, I. V. and S. V. Kovalenko (2002) C1–C5 photochemical cyclization of enediynes. *J. Am. Chem. Soc.* **120**, 9052–9053.
- Kovalenko, S. V. and I. V. Alabugin (2005) Lysine-enediyne conjugates as photochemically triggered DNA double-strand cleavage agents. *Chem. Comm.* **11**, 1444–1446.
- Yang, W.-Y., B. Breiner, S. V. Kovalenko, C. Ben, M. Singh, S. N. LeGrand, Q.-X. A. Sang, G. F. Strouse, J. A. Copland and I. V. Alabugin (2009) C-Lysine conjugates: pH-controlled light-activated reagents for efficient double-stranded DNA cleavage with implications for cancer therapy. *J. Am. Chem. Soc.* **131**, 11458–11470.
- Du, Y., C. J. Creighton, Z. Yan, D. A. Gauthier, J. P. Dahl, B. Zhao, S. M. Belkowsky and A. B. Reitz (2005) The synthesis and evaluation of 10- and 12-membered ring benzofused enediyne amino acids. *Bioorg. Med. Chem.* **13**, 5936–5948.
- Basak, A., S. S. Bag and H. M. M. Bdur (2003) Synthesis and reactivity of enediynyl amino acids and peptides: a novel concept in lowering the activation energy of Bergman Cyclisation By H-bonding and electrostatic interactions. *Chem. Commun.* **20**, 2614–2615.
- Plourde, G. II, A. El-Shafey, F. S. Fouad, A. S. Purohit and G. B. Jones (2002) Protein degradation with photoactivated enediyne-amino acid conjugates. *Bioorg. Med. Chem. Lett.* **12**, 2985–2988.
- Basak, A., S. S. Bag and A. Basak (2005) Design and synthesis of a novel enediynyl pentapeptide with predominantly b-turn structural motif and its potential as a fluorescence-based chemosensor. *Bioorg. Med. Chem.* **13**, 4096.
- Kaiser, J., B. C. J. van Esseveldt, M. J. A. Segers, F. L. van Delft, J. M. M. Smits, S. Butterworth and F. P. J. T. Rutjes (2009) Synthesis and aromatisation of cyclic enediyne-containing amino acids. *Org. Biomol. Chem.* **7**, 695–705.
- Basak, A., D. Mitra, M. Kar and K. Biradha (2008) Design, synthesis and DNA-cleaving efficiency of photoswitchable dimeric azobenzene-based C2-symmetric enediynes. *Chem. Commun.* **26**, 3067–3069.
- Fouad, F. S., J. M. Wright, G. II Plourde, A. D. Purohit, J. K. Wyatt, A. El-Shafey, G. Hynd, C. F. Crasto, Y. Lin and G. B. Jones (2005) Synthesis and protein degradation capacity of photoactivated enediynes. *J. Org. Chem.* **70**, 9789–9797.
- Breiner, B., J. C. Schlatterer, S. V. Kovalenko, N. L. Greenbaum and I. V. Alabugin (2006) Protected 32P-labels in deoxyribonucleotides: investigation of sequence selectivity of DNA photocleavage by enediyne-, fulvene-, and acetylene-lysine conjugates. *Angew. Chem. Int. Ed.* **45**, 3666–3670.
- Breiner, B., J. C. Schlatterer, S. V. Kovalenko, N. L. Greenbaum and I. V. Alabugin (2007) DNA damage-site recognition by lysine conjugates. *Proc. Natl Acad. Sci. USA* **104**, 13016–13021.
- Yang, W.-Y., Q. Cao, C. Callahan, C. Galvis, A. Q.-X. Sang and I. V. Alabugin (2010) Intracellular DNA damage by lysine-acetylene conjugates. *J. Nuc. Acids* Article ID 931394. doi:10.4061/2010/931394.
- Yang, W.-Y., S. Roy, B. Phrathep, Z. Rengert, R. Kenworthy, D. A. R. Zorio and I. V. Alabugin (2011) Engineering multiple pH-gated transitions for selective and efficient double strand DNA photocleavage in hypoxic tumors. *J. Med. Chem.* **54**, 8501–8516.
- Mohamed, R. K., P. W. Peterson and I. V. Alabugin (2013) Concerted reactions that produce diradicals and zwitterions: electronic, steric, conformational, and kinetic control of cycloaromatization processes. *Chem. Rev.* **113**, 7089–7129.
- Alabugin, I. V. and M. Manoharan (2003) Reactant destabilization in the Bergman cyclization and rational design of light- and pH-activated enediynes. *J. Phys. Chem. A* **107**, 3363–3371.
- Warburg, O. (1930) *The Metabolism of Tumors*. Constable, London.
- Tannock, I. F. and D. Rotin (1989) Acid pH in tumors and its potential for therapeutic exploitation. *Cancer Res.* **49**, 4373–4384.
- Stubbs, M., L. Rodrigues, F. A. Howe, J. Wang, K. S. Jeong, R. L. Veech and J. R. Griffiths (1994) Metabolic consequences of a reversed pH gradient in rat tumors. *Cancer Res.* **54**, 4011–4016.
- Lyons, J. C. and C. Song (1995) Killing of hypoxic cells by lowering the intracellular pH in combination with hyperthermia. *Radiat. Res.* **141**, 216–218.
- Song, C. W., J. C. Lyons, R. J. Griffin and C. M. Makepeace (1993) Thermosensitization by lowering intracellular pH with 5-(N-ethyl-N-isopropyl) amiloride. *Radiother. Oncol.* **27**, 252–258.
- Newell, K., P. Wood, I. Stratford and I. Tannock (1992) Effects of agents which inhibit the regulation of intracellular pH on murine solid tumours. *Br. J. Cancer* **66**, 311–317.

30. Kar, M. and A. Basak (2007) Design, synthesis, and biological activity of unnatural enediynes and related analogues equipped with pH-dependent or phototriggering devices. *Chem. Rev.* **107**, 2861–2890.
31. Yang, W.-Y., S. A. Marrone, N. Minors, D. A. R. Zorio and I. V. Alabugin (2011) Insights into photochemistry responsible for the double-strand DNA-cleavage via structural perturbations in diaryl alkyne conjugates. *Beilst. J. Org. Chem.* **7**, 813–823.
32. Zimmerman, H. E. (1995) The meta effect in organic photochemistry: mechanistic and exploratory organic photochemistry. *J. Am. Chem. Soc.* **117**, 8988–8991.
33. Zimmerman, H. E. and I. V. Alabugin (2001) Energy distribution and redistribution and chemical reactivity. The generalized delta overlap-density method for ground state and electron transfer reactions: a new quantitative counterpart of electron-pushing. *J. Am. Chem. Soc.* **123**, 2265–2270.
34. Albert, A. and E. P. Serjeant (1984) *The Determination of Ionization Constants*. Chapman and Hall, London.
35. Allen, R. I., K. J. Box, J. E. A. Comer, C. Peake and K. Y. Tam (1998) Multiwavelength spectrophotometric determination of acid dissociation constants of ionizable drugs. *J. Pharm. Biomed. Anal.* **17**, 699–712.
36. Martinez, C. H. R. and C. Dardonville (2013) Rapid determination of ionization constants (pKa) by UV spectroscopy using 96-well microtiter plates. *Med. Chem. Lett.* **4**, 142–145.
37. For comparison, pKa values of both compounds are higher than *p*-acetylene-lysine conjugate (pKa=6.9) and lower than lysine (pKa=8.95) itself.
38. Kumar, C. V. and E. H. Asuncion (1993) DNA binding studies and site selective fluorescence sensitization of an anthryl probe. *J. Am. Chem. Soc.* **115**, 8547–8553.
39. Kalsbeck, W. A. and H. H. Thorp (1993) Determining binding constants of metal complexes to DNA by quenching of the emission of Pt2(pop)44- (pop = P205H22-). *J. Am. Chem. Soc.* **115**, 7146–7151.
40. Suh, D. and J. B. Chaires (2007) Criteria for the mode of binding of DNA binding agents. *Bioorg. Med. Chem.* **3**, 723–728.
41. Sahoo, D., P. Bhattacharya and S. Chakravorti (2010) Quest for mode of binding of 2-(4-(Dimethylamino)styryl)-1-methylpyridinium iodide with Calf Thymus DNA. *J. Phys. Chem. B* **114**, 2044–2050.
42. Chaires, J. B. (1997) Energetics of drug–DNA interactions. *Biopolymers* **44**, 201–215.
43. LePecq, M. M. and C. Paoletti (1967) A fluorescent complex between ethidium bromide and nucleic acids: Physical-chemical characterization. *J. Mol. Biol.* **27**, 87–106.
44. Barik, A., K. I. Priyadarsini and H. Mohan (2003) Photophysical studies on binding of curcumin to bovine serum albumin. *Photochem. Photobiol.* **77**, 597–603.
45. Hiraku, Y., K. Ito, K. Hirakawa and S. Kawanashi (2007) Photosensitized DNA damage and its protection via a novel mechanism. *Photochem. Photobiol.* **83**, 205–212.
46. Steenken, S. (1989) Purine bases, nucleosides, and nucleotides: aqueous solution redox chemistry and transformation reactions of their radical cations and e- and OH adducts. *Chem. Rev.* **89**, 503–520.
47. Sugiyama, H., Y. Tsutsumi, K. Fujimoto and I. Saito (1993) Photo-induced deoxyribose C2' oxidation in DNA. Alkali-dependent cleavage of erythrose-containing sites via a retroaldol reaction. *J. Am. Chem. Soc.* **115**, 4443–4448.
48. Dunn, D. A., V. H. Lin and I. E. Kochevar (1992) Base-selective oxidation and cleavage of DNA by photochemical cosensitized electron transfer. *Biochemistry* **31**, 11620–11625.
49. Cadet, J., M. Berger, G. W. Bunchko, R. C. Joshi, S. Raoul and J.-L. Ravanet (1994) 2,2-Diamino-4-[(3,5-di-O-acetyl-2-deoxy-.beta.-D-erythro-pentofuranosyl)amino]-5-(2H)-oxazolone: a novel and predominant radical oxidation product of 3',5'-Di-O-acetyl-2'-deoxyguanosine. *J. Am. Chem. Soc.* **116**, 7403–7404.
50. Armitage, B., Y. Changjun, C. Devadoss and G. B. Schuster (1994) Cationic anthraquinone derivatives as catalytic DNA photonucleases: mechanisms for DNA damage and quinone recycling. *J. Am. Chem. Soc.* **116**, 9847–9859.
51. Saito, I. (1992) Photochemistry of highly organized biomolecules: sequence-selective photoreaction of DNA. *Pure Appl. Chem.* **64**, 1305–1310.
52. Quadda, J. C., M. J. Levy and S. M. Hecht (1993) Highly efficient DNA strand scission by photoactivated chlorobit hiazoles. *J. Am. Chem. Soc.* **115**, 12171–12172.
53. Yoshimura, Y., T. Inomata, H. Nakazawa, H. Kubo, F. Yamaguchi and T. Ariga (1999) Evaluation of free radical scavenging activities of antioxidants with an H(2)O(2)/NaOH/DMSO system by electron spin resonance. *J. Agric. Food Chem.* **47**, 4653–4656.
54. Rosenblum, W. L. and F. El-Sabban (1982) Dimethyl sulfoxide (DMSO) and glycerol, hydroxyl radical scavengers, impair platelet aggregation within and eliminate the accompanying vasodilation of, injured mouse pial arterioles. *Stroke* **13**, 35–39.
55. Devasagayam, T. P. A., S. Steenken, M. S. W. Obendorf, W. A. Schulz and H. Sies (1991) Formation of 8-hydroxy(deoxy)guanosine and generation of strand breaks at guanine residues in DNA by singlet oxygen. *Biochemistry* **30**, 6283–6289.
56. Zeidan, T., S. V. Kovalenko, M. Manoharan, R. J. Clark, I. Ghiviriga and I. V. Alabugin (2005) Triplet acetylenes as synthetic equivalents of 1,2-dicarbenes. Phantom n, π^* state controls reactivity in triplet photocycloaddition. *J. Am. Chem. Soc.* **127**, 4270–4285.
57. Zeidan, T., R. J. Clark, S. V. Kovalenko, I. Ghiviriga and I. V. Alabugin (2005) Triplet acetylenes as synthetic equivalents of 1,2-dicarbenes. II. New supramolecular scaffolds from photochemical cycloaddition of diarylacetylenes to 1,4-cyclohexadienes. *Chemistry Eur. J.* **11**, 4953–4962.